MauG, a Novel Diheme Protein Required for Tryptophan Tryptophylquinone Biogenesis[†]

Yongting Wang,[‡] M. Elizabeth Graichen,[‡] Aimin Liu,[‡] Arwen R. Pearson,[§] Carrie M. Wilmot,[§] and Victor L. Davidson*,[‡]

Department of Biochemistry, University of Mississippi Medical Center, Jackson, Mississippi 39216, and Department of Biochemistry, Molecular Biology, and Biophysics, University of Minnesota, Minneapolis, Minnesota 55455

Received February 12, 2003; Revised Manuscript Received April 9, 2003

ABSTRACT: The biosynthesis of methylamine dehydrogenase (MADH) from *Paracoccus denitrificans* requires four genes in addition to those that encode the two structural protein subunits. None of these gene products have been previously isolated. One of these, *mauG*, exhibits sequence similarity to diheme cytochrome *c* peroxidases and is required for the synthesis of the tryptophan tryptophylquinone (TTQ) prosthetic group of MADH. A system was developed for the homologous expression of MauG in *P. denitrificans*. Its signal sequence was correctly processed, and it was purified from the periplasmic cell fraction. The protein contains two covalent *c*-type hemes, as predicted from the deduced sequence. EPR spectroscopy reveals that the protein as isolated possesses about equal amounts of one high-spin heme with axial symmetry and one low-spin heme with rhombic symmetry. The low-spin heme contains a major and minor component suggesting a small degree of heme heterogeneity. The high-spin heme and the major low-spin heme component each exhibit resonances that are atypical of *c*-type hemes and dissimilar to those reported for diheme cytochrome *c* peroxidases. MauG exhibited only very weak peroxidase activity when assayed with either *c*-type cytochromes or *o*-dianisidine as an electron donor. Fully reduced MauG was shown to bind carbon monoxide and could be reoxidized by oxygen. The relevance of these unusual properties of MauG is discussed in the context of its role in TTQ biogenesis.

Paracoccus denitrificans is a Gram-negative bacterium that is able to grow under a wide variety of conditions (*1*). When grown on methylamine as a sole source of carbon and energy, the initial step in the metabolism of methylamine is its oxidative deamination by a periplasmic methylamine dehydrogenase (MADH)[1] (*2*). MADH exhibits a heterotetrameric $\alpha_2\beta_2$ structure (*3*), and each β subunit of MADH possesses a tryptophan tryptophylquinone (TTQ) cofactor (*4*) that is formed by posttranslational modification. During this modification, two oxygens are incorporated into βTrp^{57}, and a cross-link is formed between βTrp^{57} and βTrp^{108} (Figure 1). It is believed that TTQ biogenesis is a multistep process that involves oxygenation of βTrp^{57} followed by cross-linking, possibly by nucleophilic attack from βTrp^{108} (*4*, *5*). Studies of model compounds revealed that it was possible to synthesize TTQ by first forming a dioxygenated quinone and then cross-linking (*6*). The biosynthesis of the TTQ cofactor requires the action of at least one other gene product (*7*, *8*). This contrasts TTQ enzymes with the well-known class of quinoprotein copper-containing amine oxidases in which the posttranslational modification of tyrosine to form the topa quinone (TPQ) cofactor is a self-processing mechanism involving a bound copper and molecular oxygen (*5*, *9*).

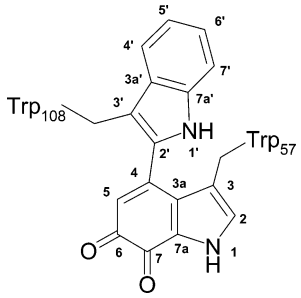

FIGURE 1: Structure of tryptophan tryptophylquinone (TTQ).

The genes encoding the α and β subunits of MADH are located in the methylamine utilization (*mau*) gene cluster (*10*). The *mau* cluster of *P. denitrificans* has 11 genes with a gene order of *mauRFBEDACJGMN* (*7*). The *mau* clusters that have been characterized from three other methylotrophic bacteria have similar compositions (*11*−*13*). The first gene, *mauR*, is a LysR-type transcriptional activator (*14*). The α and β subunits of MADH are encoded by *mauB* and *mauA*, respectively, and *mauC* (*15*) encodes the blue copper protein, amicyanin, which serves as the obligate electron acceptor of MADH (*16*). Four other genes, which are conserved in all *mau* gene clusters, have been shown to be essential for MADH biosynthesis in *P. denitrificans*. Deletions of either *mauF* (*7*), *mauD* (*8*), *mauE* (*8*), or *mauG* (*7*) result in loss

[†] This work was supported by NIH Grants GM-41574 (V.L.D.) and GM-66569 (C.M.W.). A.L. acknowledges generous faculty start-up funds from the University of Mississippi Medical Center.

* To whom correspondence should be addressed. Tel: 601-984-1516. Fax: 601-984-1501. E-mail: vdavidson@biochem.umsmed.edu.

[‡] University of Mississippi Medical Center.

[§] University of Minnesota.

[1] Abbreviations: MADH, methylamine dehydrogenase; TTQ, tryptophan tryptophylquinone; TPQ, topaquinone; EPR, electron paramagnetic resonance; CCP, cytochrome *c* peroxidase; ESI, electrospray ionization; TOF, time of flight.

10.1021/bi034243q CCC: $25.00
Published on Web 05/24/2003

of both MADH activity and the ability of the bacterium to grow on methylamine. For the first three deletions, no MADH protein was detected in cell extracts. In contrast, the results of *mauG* deletion studies in *P. denitrificans* suggested that MauG is specifically involved in TTQ maturation. While the cells with the *mauG* deletion were lacking in MADH activity and were unable to grow on methylamine as the sole carbon source, it was shown by Western blot analysis that near wild-type levels of the MADH β subunit were expressed (*7*). Furthermore, upon the addition of methylamine these cell extracts did not exhibit the characteristic fluorescence associated with aminoquinol formation during catalytic turnover in wild-type cells. This suggested that the quinone cofactor was not fully biogenesized in the *mauG* deleted strain (*7*). Similar results were obtained from *mauG* deletion studies in *Methylobacterium extorquens* AM1 (*11*).

Analysis of the sequence of *mauG* reveals a putative signal sequence, consistent with the periplasmic location of MADH, and two heme *c* binding motifs (CXXCH). The sequence also shows about 30% similarity to those of bacterial diheme cytochrome *c* peroxidases. Although MADH and amicyanin may be isolated in relatively large yield from the periplasmic fraction of *P. denitrificans* that has been grown on methylamine as a carbon source (*17*), it has not been possible to isolate MauG from these cell extracts. In this paper, we describe the design of a homologous expression system for the purification of recombinant MauG from *P. denitrificans*. The physical, kinetic, and spectroscopic properties of MauG are described. These results suggest that MauG represents a unique class of diheme proteins with novel reactivity that is consistent with a role in TTQ biogenesis.

EXPERIMENTAL PROCEDURES

Construction of Plasmids for MauG Expression. Routine cloning steps were performed using restriction enzymes purchased from New England Biolabs, plasmid miniprep kits from Marligen Biosciences, Ready-to-Go T4 DNA ligase from Amersham Pharmacia, and competent JM109 cells from Promega. *Escherichia coli* strains were cultured in LB media or on LB agar at 37 °C. The plasmid pMAU38-2 was provided by R. J. M. van Spanning (Vrije Universiteit, Amsterdam), and pEC86 was provided by L. Thony-Meyer (ETH Zurich).

The plasmid pMAU38-2 is derived from the pBluescript II KS(+) vector (Stratagene). It contains *mauG* with a point mutation creating an *Nde*I site at the starting ATG codon to allow fusion with the promoter region from the *cycA* (cytochrome *c*-550) gene of *P. denitrificans* (*18*). A hexahistidine tag was inserted at the C-terminal of *mauG* by site-directed mutagenesis using the Stratagene QuikChange kit. To introduce the insertion, the standard protocol was modified by the addition of 10% DMSO and 2% dimethylformamide to the polymerase reaction. In this reaction, pMAU38-2 was used as the template, and the primers that were used were 5′-CCGCTGCTGGAGGAAAGCCGCGCGGCGCAAAAGGACCACCACCACCACCACCACTGACCAAGGGCCCCCGCCGGG-3′ and its complementary DNA. The bases encoding the His_6 tag are underlined. The insertion was confirmed by DNA sequencing. The *cycA*pr-*mauG*-6xHis segment was excised with *Xba*I and ligated into pRK415-1, a broad-host-range vector of the P1 incompatibility group (*19*) to create pMEG391. This plasmid was introduced into *P. denitrificans* by conjugation with the mobilizing *E. coli* strain S17-1. Due to instability of the plasmid in *P. denitrificans* (*20*), it was necessary to reintroduce the plasmid into fresh cells every 6−8 weeks.

Purification of MauG. To express the MauG protein, *P. denitrificans* cells (ATCC 13543) containing pMEG391 were grown aerobically, at 30 °C, in mineral salts medium (*21*) supplemented with 0.6 mM $NaHCO_3$, 1.6 μM $CuSO_4$, 0.5 g/L yeast extract, 34 mM succinate, and 2 μg/mL tetracycline. After harvest of the cells by centrifugation, the periplasmic cell fraction was isolated as described previously using a lysozyme−osmotic shock method (*22*). The procedure was modified as follows so that the His_6-tagged protein could be isolated directly from the periplasmic fraction without dialysis or concentration of the periplasm. Cells were suspended (5 mL/g wet weight cells) in 50 mM sodium phosphate, pH 8.0, with 0.5 M sucrose and 0.67 mM EDTA. The suspension was incubated with lysozyme (7.5 mg/g wet weight cells) at 30 °C for 15 min. The protease inhibitor phenylmethanesulfonyl fluoride (0.15 mM) was added, and the cells were subjected to a mild osmotic shock by addition of an equal volume of water. After 45 min of further incubation at 30 °C, 0.5 mM $MgCl_2$ (to chelate the EDTA) and 300 mM NaCl were added, and the mixture was centrifuged at 25000*g* for 35 min. To the supernatant (periplasm) was added 20 mL of Ni-NTA Superflow resin (Qiagen). This mixture was stirred slowly for 30 min at 4 °C and then poured into a chromatography column to isolate the resin. The resin was washed with 50 mM sodium phosphate, pH 8.0, containing 300 mM NaCl and then a gradient of increasing concentration of imidazole in this buffer. The His_6-tagged MauG protein eluted from the Ni-NTA resin in 70 mM imidazole. The average yield of purified MauG is about 5 mg/100 g wet weight cells.

Electrophoretic Analysis. SDS−polyacrylamide gel electrophoresis was performed by standard methods using 12.5% gels. Gels were stained for protein with Coomassie Blue G250. Specific staining of proteins with covalently bound heme was performed according to the protocol of Francis and Becker (*23*). Western blot analysis of these gels was performed with monoclonal antibody to the His_6 tag (Clonetech).

N-Terminal Protein Sequencing. MauG samples were electrophoresed on a NuPage 4−12% Bis-Tris gel (Invitrogen) and then blotted onto BioTrace PVDF membrane (Pall Gelman Sciences) using an XCell II blot module (Invitrogen) according to the manufacturer's protocol. Protein was visualized using 0.1% (w/v) amido black in 40% (v/v) methanol, and the membrane was air-dried. N-Terminal sequencing was carried out using an automated HP241 protein sequencing system (Hewlett-Packard).

Mass Spectrometry. MauG samples were desalted using 20 μm Porus R2 resin (polystyrene divinylbenzene) [Applied Biosystems, Inc. (ABI)] in a glass purification capillary. The sample was loaded onto the R2 resin, washed three times with ~7 μL of 5% acetonitrile plus 0.5% formic acid, and eluted with ~1.5 μL of 70% acetonitrile plus 0.5% formic acid into a coated nanoelectrospray capillary.

Electrospray ionization (ESI) mass spectra were acquired using a QSTAR pulsar *i* (ABI) quadrupole-TOF (time of flight) mass spectrometer equipped with a nano-ESI source

(Protana Engineering, Denmark). The ESI voltage was 1000 V, the TOF region acceleration voltage was 4 kV, and the injection pulse repetition rate was 6.0 kHz. External calibration was performed using human angiotensin II (monoisotopic mass [MH^+] 1046.5417 Da; Sigma) and adrenocorticotropin hormone fragment 18−39 (monoisotopic mass [MH^+] 2465.1989 Da; Sigma). Mass spectra were the average of approximately 300 scans collected in the positive mode over a 5 min acquisition period. The series of multiply charged protein peaks were deconvoluted to provide protein zero-charge mass using the Bayesian Reconstruct tool in the ABI BioAnalyst software package, which is based on maximum entropy theory.

UV−Visible Spectroscopic Analysis. UV−visible spectra were obtained with a Shimadzu MultiSpec-1501 spectrophotometer. Reduction of MauG was performed anaerobically by titration with sodium dithionite. CO binding to reduced MauG was determined by recording the absorption spectrum 2 min after CO was bubbled into the dithionite-reduced solution of MauG. Extinction coefficients were measured by the pyridine hemochrome method (*24*).

EPR Spectroscopic Analyses. First derivative EPR spectra were collected at X-band microwave frequency and 100 kHz field modulation with a Bruker E-500 spectrometer. A calibrated frequency counter and a Bruker ER035M NMR gauss meter were used for the *g*-value determinations. The low-temperature (2−50 K) measurements were achieved with an Oxford Instruments ESR-10 continuous flow liquid helium cryostat and a digitalized temperature controller. Spin quantitation was performed by double integration of each of the resonances acquired under nonsaturating conditions at 20 K using a Cu-EDTA standard (1 mM) for calibration. The EPR relaxation behavior was studied by recording spectra at different microwave powers and at different temperatures. The microwave power at half-saturation parameter $P_{1/2}$ was obtained as described in the literature (*25*, *26*).

Kinetic Analysis. Dye-linked peroxidase activity was assayed in 0.15 M citrate−phosphate buffer, pH 5. The reaction mixture included 0.1 mM *o*-dianisidine and either 20 nM MauG or 0.3 nM horseradish peroxidase. The latter was used as a positive control. Reactions were initiated by addition of 1 mM H_2O_2. The reaction was monitored by the increase in the absorbance at 460 nm caused by the oxidation of *o*-dianisidine. Cytochrome *c* peroxidase activity of MauG was assayed in either 10 mM potassium phosphate buffer, pH 7, or 5 mM MES−HEPES buffer, pH 6. Reactions were assayed using commercial horse heart cytochrome *c* (Sigma) or *P. denitrificans* cytochromes *c*-550 or *c*-551i (*27*) as electron donors. The *P. denitrificans* cytochromes were purified as described previously (*27*). The cytochromes were reduced with ascorbate, and excess reductant was removed by passage over Sephadex G-25. Reactions were initiated by addition of 1 mM H_2O_2. The activity was monitored by the decrease in the absorbance at the α-band caused by the oxidation of the ferrocytochrome *c*.

RESULTS

Expression of MauG. Attempts to express MauG in heterologous expression systems using *E. coli* and *Rhodobacter sphaeroides* were made but met with very limited success. These attempts will be briefly summarized. For expression in *E. coli*, constructs containing the His_6-tagged *mauG* were prepared using the commercial plasmids pET20b and pBluescript II. Expression was tried in BL21(DE3) and BL21-CodonPlus (DE3)-RP (Stratagene) cells. The maximum levels of protein that were isolated totaled less than 1 mg of His_6-tagged MauG per 100 g wet weight of cells. Expression of *c*-type cytochromes in *E. coli* is known to be problematic. Since MauG was believed to possess two covalent *c*-type hemes, attempts were also made to express *mauG* in *E. coli* cells that had been cotransformed with a second plasmid, pEC86, which possesses genes that are required for cytochrome *c* maturation (*28*). However, this gave no improvement. MADH has been successfully expressed in *R. sphaeroides* in a pRK415-1 vector which contains the *mau* genes necessary for MADH biosynthesis under the control of the *coxII* promoter from that bacterium (*29*). An analogous *coxII* promoter-*mauG*-His_6 construct was prepared in pRK415-1 and introduced into *R. sphaeroides*. Under growth conditions which have been used for heterologous expression of MADH, there was no detectable His_6-tagged MauG.

Homologous expression of recombinant His_6-tagged MauG was achieved in *P. denitrificans* as described under Experimental Procedures. Cells were grown on succinate as a carbon source. Under these growth conditions, MADH is not expressed (*30*). Using the method described under Experimental Procedures, the purified MauG was isolated from the freshly prepared periplasmic fraction in about 3 h. The average yield was about 5 mg per 100 g wet weight of cells. Attempts were also made to express *mauG* in *P. denitrificans* using an identical construct that lacked the hexahistidine tag. It was not possible to identify or isolate any untagged MauG from the periplasm of these cells. This may be a reflection of the instability of MauG in crude extracts during the purification process. This also may explain why it has not been possible to isolate native MauG from extracts of *P. denitrificans* after growth on methylamine. It might be expected that a protein involved in biogenesis of an enzyme would have a short half-life and be rapidly degraded once it had completed its task. Consistent with this notion is the observation that if the periplasm is concentrated and dialyzed prior to addition of the affinity resin, the yield is much less than when the resin is added immediately in our modified protocol. The addition of the His_6 tag and the modified purification protocol have dramatically improved the yield of MauG by allowing for more rapid purification from cellular extracts and possibly also by increasing the resistance of the protein to degradation.

Protein Analysis. The purified MauG protein migrates as a single band during SDS−PAGE with an apparent mass of 42 kDa. The band stains positively for heme and exhibits a positive reaction after Western blot and incubation with monoclonal antibody to the His_6 tag. N-Terminal amino acid sequencing indicated that the first 10 amino acid residues of this protein are EQARPADDAL. This sequence exactly matches that predicted from the *mauG* sequence after removal of the putative signal sequence, which is also predicted from the gene sequence. The exact mass of the expressed protein was determined by mass spectrometry. The predicted mass for the His_6-tagged MauG polypeptide is 41087.7 Da. After covalent addition of two hemes, the mature

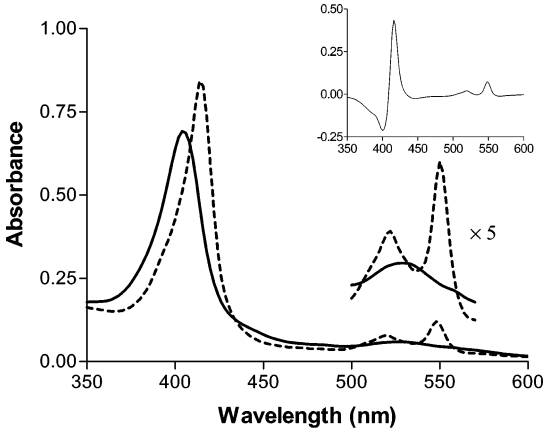

FIGURE 2: Absorption spectra of fully oxidized and reduced MauG. MauG was present at a concentration of 3.0 μM in 50 mM BTP buffer (pH 7.5). The spectrum of the oxidized MauG (solid line) is that of the protein as isolated, and the spectrum of the reduced MauG (broken line) was obtained after addition of sodium dithionite. The reduced minus oxidized difference spectrum is shown in the inset.

protein is expected to have a mass of 42319.7 Da. ESI yielded a mass of 42321.5 ± 0.7 Da. These data indicate that the purified MauG protein has been correctly processed and assembled, possesses two covalent hemes, and contains no additional modifications.

UV−Visible Spectroscopic Properties. The UV−visible absorption spectra of the fully oxidized and reduced forms of MauG are shown in Figure 2. The protein as isolated was in the oxidized form and exhibited a Soret band absorbance maximum at 406 nm and a broad absorbance feature centered at 526 nm. Incubation of the protein with ferricyanide caused no change in the absorption spectrum. Anaerobic titration with dithionite yielded the fully reduced MauG, which exhibited absorbance maxima at 416, 524 (β), and 552 (α) nm. Intermediate forms were difficult to distinguish during the reductive titration with dithionite. The titration required two electron equivalents for complete reduction. Isosbestic points were maintained during the titration. The heme concentration that was determined by the pyridine hemochrome method was used to determine the following extinction coefficients. The value for oxidized MauG is ϵ_{406} = 207.6 mM^{-1} cm^{-1}. The values for reduced MauG are ϵ_{416} = 232.9 mM^{-1} cm^{-1}, ϵ_{524} = 25.3 mM^{-1} cm^{-1}, and ϵ_{552} = 31.6 mM^{-1} cm^{-1}.

It was observed that reduced MauG was able to react directly with molecular oxygen. Dithionite-reduced MauG was reoxidized by exposing the protein solution to air. The spectra in Figure 3 were obtained before and 2.5 h after exposing the anaerobic solution of reduced MauG to room air. The initial sample contained an excess of dithionite to ensure complete reduction of MauG prior to exposure to air. If air is introduced more rapidly into the solution, by bubbling, then the spectral changes are complete within a few minutes. The final reoxidized form of MauG shows the same spectral features as the original MauG, as isolated, except that the intensity of the Soret peak is diminished. The reason for this is not clear.

The reduced form of MauG was also shown to bind carbon monoxide. The spectral changes caused by CO binding are shown in Figure 4. The Soret band blue shifts from 416 to 414 nm and exhibits an increase in extinction coefficient. In

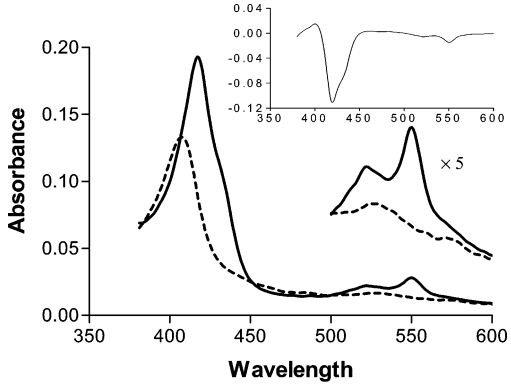

FIGURE 3: Reoxidation of MauG by air. MauG was present at a concentration of 0.8 μM in 50 mM BTP buffer (pH 7.5). Absorption spectra were recorded of dithionite-reduced MauG before (solid line) and after (broken line) exposure to room air. A slight excess of dithionite was present at the beginning of the experiment to ensure full reduction of MauG. The air-oxidized minus reduced difference spectrum is shown in the inset.

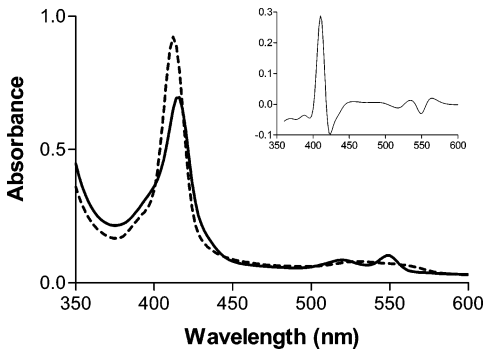

FIGURE 4: Absorption spectra of reduced MauG in the presence and absence of CO. MauG was present at a concentration of 3.0 μM in 50 mM BTP buffer (pH 7.5). Spectra were recorded of dithionite-reduced MauG before (solid line) and after (broken line) equilibration with CO. The reduced plus CO minus reduced difference spectrum is shown in the inset.

the visible region, CO binding causes both α- and β-bands (552 and 524 nm, respectively) to broaden. The reactivity of CO-bound reduced MauG to oxygen was also examined. After exposure to air, the spectrum of the CO-bound reduced MauG was converted to that of the original oxidized protein (not shown), indicating that air is able to fully reoxidize CO-bound, reduced MauG. This reaction occurred on approximately the same time scale as the reaction of reduced MauG with air.

Certain properties of the diheme cytochrome *c* peroxidase of *P. denitrificans* are affected by Ca^{2+} (*31*, *32*). Possible effects of Ca^{2+} on the spectral properties of MauG were examined. A dithionite titration of MauG was performed in the presence of 1 mM $CaCl_2$. The presence of Ca^{2+} in the system had no significant effect on the features of the initial or final spectrum or on the rate of reduction.

EPR Spectroscopic Properties. EPR spectra of oxidized MauG obtained at 10 and 40 K are shown in Figure 5. The MauG EPR signals are comprised of two types of ferric heme, with one high-spin and one low-spin state. Each of the spin states accounts for about half of the total spin concentration, consistent with MauG being a diheme protein with two distinct hemes. The EPR spectrum at 10 K shows three distinct spectral components. One set of resonances at $g_\perp$ = 5.57 and $g_\parallel$ = 1.99 originated from a high-spin (S =

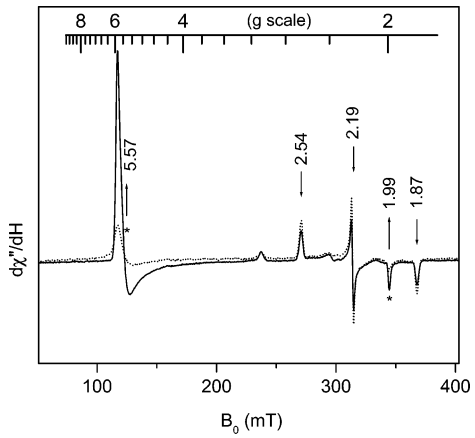

FIGURE 5: X-band EPR spectra of oxidized MauG in its as-isolated form at pH 7.5. A sample of the as-isolated MauG (120 μM) in 10 mM potassium phosphate buffer (pH 7.5), plus 5% glycerol, was transferred into a 4 mm quartz EPR tube and chilled by liquid nitrogen prior to the EPR measurements. The solid trace was obtained at 10 K, and the dotted line was obtained at 40 K. Each of the traces is the average of three scans. Both the magnetic field and *g*-scale are presented. For clarity, the high-spin resonances (species I) are indicated with stars. The instrumental conditions were 0.1 mW microwave power, 1 mT modulation, 0.082 s time constant, and 3 mT/s sweep rate.

$^5/_2$) ferric heme with nearly pure axial symmetry (species I). Two sets of resonances characteristic of low spin ($S = {}^1/_2$) ferric centers were also detected, corresponding to two populations of rhombic low-spin heme. The major component (species II) exhibits sharp resonances at $g_z = 2.54$, $g_y = 2.19$, and $g_x = 1.87$, and this is typical of hexacoordinated low-spin heme with almost pure rhombic symmetry. A minor component (species III) with axial-distorted rhombic symmetry that exhibits resonances at $g_z = 2.89$, $g_y = 2.32$, and $g_x = 1.52$ (a broad feature; not shown) is also present in the spectrum (species III). The ratio of concentrations of species II to species III was estimated to be approximately 5 to 1 from the relative line intensity of the peaks at 20 K (not shown). The three species have distinct temperature dependencies and relaxation properties. The high-spin species I was best observed by EPR at low temperatures (i.e., 2−10 K), and its signal intensity decreased as temperature increased. The intensity of the EPR signal of the major low-spin component (species II) was maximal around 20 K. The minor species III was relatively insensitive to changes in temperature. At 20 K, the high-spin species cannot be saturated by microwave power readily available up to 200 mW, indicating that the unpaired electron spins are mostly centered on the ferric ion itself. In contrast, the $P_{1/2}$ values of species II and III are 0.7 and 0.08 mW, respectively. These results indicate that the major and minor low-spin heme species are experiencing different protein environments. This suggests that a small percentage of the MauG population may be present in a somewhat different conformation which alters the environment of the low-spin heme.

Peroxidase Activity. Since the sequence of MauG shows some similarity to those of diheme cytochrome *c* peroxidases, MauG was examined for peroxidase activities. Cytochrome *c* peroxidase activity was assayed using three different cytochromes as potential electron donors. No activity was detected with *P. denitrificans* cytochrome *c*-550. Very low levels of activity were detected with *P. denitrificans* ferrocytochrome *c*-551i and horse heart ferrocytochrome *c*, with turnover numbers of 72 and 240 min^{-1}, respectively. By comparison, *P. denitrificans* cytochrome *c* peroxidase exhibits turnover numbers of 85000 and 62000 min^{-1} for the reactions with *P. denitrificans* ferrocytochrome *c*-550 and horse heart ferrocytochrome *c*, respectively (*32*). MauG was also assayed for general peroxidase activity with *o*-dianisidine as an electron donor. Again, weak peroxidase activity was observed with a turnover number of 64 min^{-1}. For comparison, the reaction was repeated using horseradish peroxidase as a positive control. The turnover number for that reaction was 65000 min^{-1}.

DISCUSSION

It has been known for several years that *mauG* is required for MADH biogenesis (*7*, *11*). From analysis of its deduced sequence, possible features of its structure and possible roles in TTQ biosynthesis have been proposed. In this paper, we report the successful expression and purification of MauG and describe several of its fundamental properties. Two important structural features that were predicted from the sequence have been confirmed. The putative signal sequence was correctly predicted, and it is processed at the predicted site. Also, consistent with the sequence analysis is the presence of two covalent *c*-type hemes. This is confirmed by mass spectrometry and EPR spectroscopic analysis. MauG also exhibits some unexpected properties which distinguish it from other *c*-type heme proteins. Despite its similarity to diheme cytochrome *c* peroxidases, MauG does not function well as a peroxidase, although one cannot rule out the possibility that it may possess a higher peroxidase activity with its natural substrates. MauG also exhibits EPR properties that are different from those of diheme cytochrome *c* peroxidases and from *c*-type heme proteins in general. MauG exhibits reactivity toward CO and molecular oxygen when reduced, a property not typical of *c*-type cytochromes. This raises the possibility that MauG may be an oxygenase and that the reduced form of the enzyme is involved in TTQ biogenesis. This would fit with a role for MauG in oxygen incorporation into the TTQ cofactor.

In Figure 6, the amino acid sequence of the MauG from *P. denitrificans* (*7*) is compared with the deduced sequences of MauG proteins from *M. extorquens* AM1 (*11*) and *Methylophilus methylotrophus* (*12*) and sequences of diheme cytochrome *c* peroxidases from *P. denitrificans* (*33*), *Pseudomonas aeruginosa* (*34*), and *Nitrosomonas europaea* (*35*). In contrast to the high similarity of 61% between the *P. denitrificans* and *P. aeruginosa* cytochrome *c* peroxidase, the sequence similarity between MauG of *P. denitrificans* and other MauG proteins is low. However, the MauG proteins from the more closely related methylotrophic bacteria, *M. extorquens* AM1 and *M. methylotrophus*, show a similarity of 53%. In general, the similarity between MauG proteins and diheme cytochrome *c* peroxidases is low. It is also interesting to note that the conserved methionine and histidine residues which are seen in the crystal structures to serve as the sixth ligands for the hemes in the cytochrome *c* peroxidases (*34*, *36*) are not in the corresponding positions in the alignment with MauG sequences (Figure 6). This sequence analysis suggests that MauG proteins should be classified as a distinct class of diheme proteins rather than a new class of cytochrome *c* peroxidases.

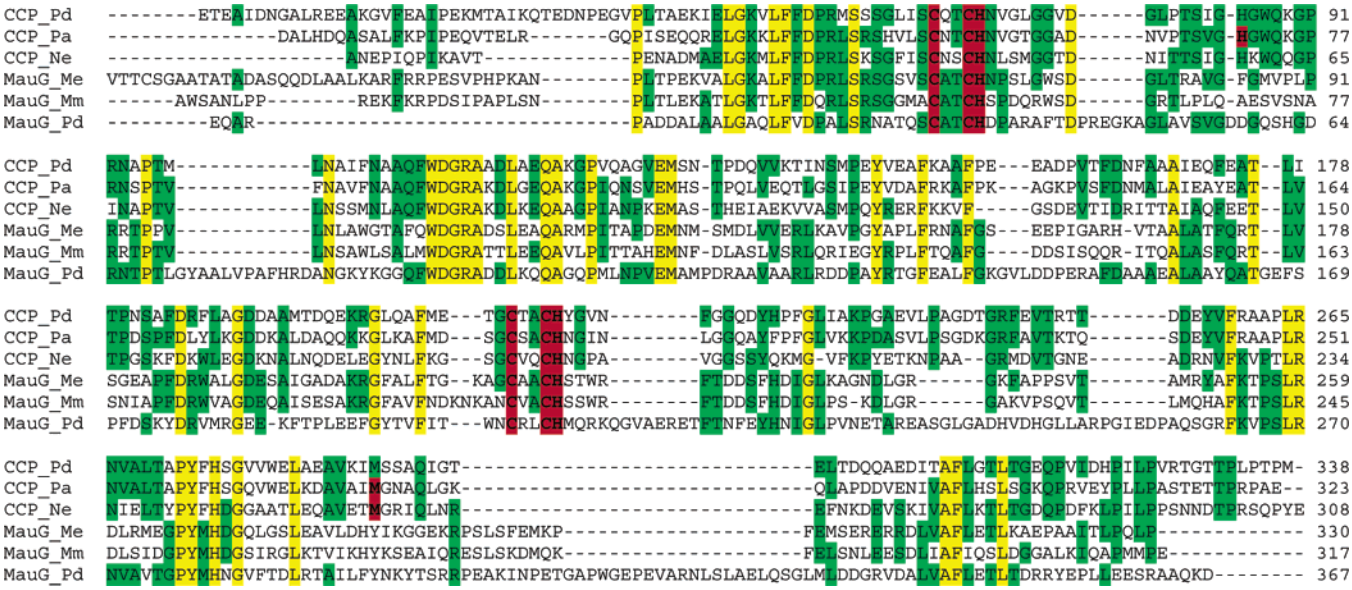

FIGURE 6: Comparison of the amino acid sequences of MauG from *P. denitrificans* (MauG_Pa), *M. extorquens* AM1 (MauG_Me), and *M. methylotrophus* (MauG_Mm) with sequences of cytochrome *c* peroxidase from *P. denitrificans* (Ccp_Pd), *Ps. aeruginosa* (Ccp_Pa), and *N. europaea* (CCP_Ne). Alignment was done using the ClustalW program provided by European Bioinformatics Institute (EBI, http://www.ebi.ac.uk/clustalw/); the matrix used is BLOSUM. Align parameters are as follows: gap open = 10, gap extension = 0.05, and gap distance = 8. Residues are highlighted in yellow if they are identical in every sequence. If the residue is identical in 3−5 sequences it is highlighted in green. The conserved cysteines and axial histidine that are predicted by the CXXCH binding motif are in red. The H and M residues which provide sixth ligands in the crystal structures of CCP_Pa (*34*) and CCP_Ne (*36*) are also in red. The crystal structure of CCP_Ne shows that His59 is not in a position for it to serve as a ligand. The authors argue that this sixth position is open in the oxidized form, which is the reason this CCP is active in its oxidized form. In contrast, CCP_Pd is active in the mixed valence state.

Table 1: Comparison of EPR Parameters of MauG with Those of Diheme Cytochrome *c* Peroxidases

enzyme (redox state)	high spin ($S = {}^5/_2$) g_z, g_y, g_x	low spin ($S = {}^1/_2$) g_z, g_y, g_x	ref
P. denitrificans MauG (oxidized)	5.57, 5.57, 1.99	2.54, 2.19, 1.87 (major) 2.89, 2.32, 1.52 (minor)	this work
P. denitrificans CCP (oxidized)	6, ?, ?[a] (minor species)[b]	3.00, 2.27, 1.44	*38*
P. denitrificans CCP (active + Ca^{2+})[c]		2.89, 2.32, 1.51	*38*
Ps. aeruginosa CCP (oxidized)		3.00, ?, ? 3.27, ?, ?	*39*
Ps. aeruginosa CCP (active)		2.85, 2.36, 1.54 3.00, 2.26, ?	*39*
N. europaea CCP (oxidized)	6.26, 5.75, 1.99	2.86, 2.38, 1.49 2.81, 2.38, 1.55	*40*

[a] ? indicates not reported. [b] The majority of the high-spin heme showed up as a low-spin heme at cryogenic temperature with an observed $g_z = 3.41$ and estimated $g_y = 2.0$ and $g_x = 0.6$ resonances. The weak $g = 6$ resonance represents a minor ferric heme component (*38*). [c] Active refers to the mixed valence form of CCP (*37*). The *P. denitrificans* enzyme requires Ca^{2+} for this form to be active.

EPR spectroscopy provides unequivocal evidence for a diheme redox pair in $Fe(III)_2$ MauG, one high-spin Fe with axial symmetry and the other in low spin with predominantly rhombic symmetry. The simultaneous EPR observation of high-spin and low-spin ferric cytochromes, described for oxidized MauG, is very unusual. In the *c*-type diheme peroxidases that have been characterized, the majority of the high-spin heme usually undergoes a temperature-dependent high-spin to low-spin interconversion (spin transition). This in turn results in an EPR spectrum dominated by only low-spin ferric signals (Table 1) (*37*−*40*). The *g*-values for the EPR signals of the high-spin heme of MauG are also dissimilar to those of the diheme *c*-type cytochrome *c* peroxidases (Table 1) and more similar to those of other types of heme proteins (Table 2). A review of the literature reveals that the high-spin heme signal of MauG is very similar to that of the bound-heme substrate in the heme oxygenase−heme complex (*41*) and more similar to myoglobin (*42*) than to the diheme peroxidases.

The observation of two low-spin ferric centers reveals some heme heterogeneity for the MauG low-spin heme. The major low-spin component, species II, exhibits *g*-values that are unusual for a *c*-type heme (Table 1) and more similar to those of other types of heme proteins (Table 2). These include some ligand complexes of P450cam (*43*−*46*) and chloroperoxidase (*47*), the pyridoxal phosphate-dependent heme enzyme human cystathionine β-synthase (*48*), and the verdoheme complex with heme oxygenase-1 obtained by addition of H_2O_2 (*49*). The minor species III exhibits *g*-values that are nearly identical to those of the diheme cytochrome *c* peroxidases (Table 1) and which may account for the observed low level of peroxidase activity.

The characterization of MauG as an oxygen-binding protein further distinguishes it from peroxidases and supports an atypical role for at least one of the *c*-type hemes of MauG. Oxygen binding is not a common feature for a protein that contains *c*-type heme. Myoglobin and hemoglobin both contain protoheme instead of a *c*-type heme. At least two

Table 2: Examples of Heme Proteins with EPR Resonances Similar to Those of MauG

enzyme	low spin ($S = 1/2$) g_z, g_y, g_x	ref
P. denitrificans MauG	2.54, 2.19, 1.87	this work
cystathionine β-synthase	2.50, 2.30, 1.86	*48*
heme oxygenase-1 + heme + H_2O_2	2.57, 2.14, 1.86	*49*
P450cam + imidazole	2.56, 2.27, 1.87	*43*
P450cam + *N*-methylimidazole	2.54, 2.26, 1.87	*44*
P450cam + CH_3SCH_3	2.50, 2.27, 1.89	*45*
P450cam + formate	2.55, 2.25, 1.88	*46*
chloroperoxidase + imidazole	2.54, 2.28, 1.85	*47*

enzyme	high spin ($S = 5/2$) $g_\perp$, $g_\parallel$	ref
P. denitrificans MauG	5.57, 1.99	this work
heme oxygenase + heme	5.62, 2.00	*41*
heme oxygenase H20A mutant + heme	5.68, 2.00	*41*
myoglobin	5.92, 1.99	*42*

other oxygen-binding *c*-type heme proteins have been characterized. These are *sphaeroides* heme protein (SHP) from *R. sphaeroides* (*50*) and oxygen-binding heme protein from *Chromatium vinosum* (*51*). The physiological significance of oxygen binding to *c*-type cytochromes is not known. For MauG, however, the fact that its heme binds oxygen is consistent with its potential role in oxygen incorporation into tryptophan during TTQ biosynthesis. Together with the observation that MauG exhibits very low peroxidase activity, these results suggest that MauG functions in TTQ biosynthesis by a mechanism other than that of a typical peroxidase.

The biogenesis of TTQ in MADH requires insertion of two oxygens into βTrp^{57} and formation of a covalent cross-link between the indole rings of βTrp^{57} and βTrp^{108}. Mutational studies have indicated that MauG is required for this process (*7*, *11*). Although MauG has previously been suggested to be a diheme cytochrome *c* peroxidase, on the basis of sequence similarity, it was not clear how such a peroxidase activity would be applicable to reactions required for the biogenesis of TTQ. An oxygenase activity would seem to be more relevant. As such, the reactivity of MauG with oxygen and the similarity of the EPR signals of MauG with oxygen-binding proteins and oxygenases are intriguing. More detailed spectroscopic and redox studies are planned to more fully characterize this unusual diheme protein, and attempts to crystallize MauG have been initiated.

ACKNOWLEDGMENT

We thank Dr. John D. Lipscomb at the University of Minnesota for access to the EPR facility, Dr. Rob van Spanning at Vrije Universiteit in Amsterdam for providing us with plasmids containing *mauG* and the *cycA* promoter, Dinesha Walek, Sudha Marimanikkuppam, Yu Tang, and Benjie Mangilog for technical support, and Drs. Jon Hosler and Brian Brazeau for helpful advice and comments.

REFERENCES

1. John, P., and Whatley, F. R. (1977) *Biochim. Biophys. Acta 463*, 129−153.
2. Davidson, V. L. (2001) *Adv. Protein Chem. 58*, 95−140.
3. Chen, L., Doi, M., Durley, R. C., Chistoserdov, A. Y., Lidstrom, M. E., Davidson, V. L., and Mathews, F. S. (1998) *J. Mol. Biol. 276*, 131−149.
4. McIntire, W. S., Wemmer, D. E., Chistoserdov, A., and Lidstrom, M. E. (1991) *Science* 252, 817−824.
5. Schwartz, B., and Klinman, J. P. (2001) *Vitam. Horm. 61*, 219−239.
6. Itoh, S., Ogino, M., Haranou, S., Terasaka, T., Ando, T., Komatsu, M., Oshiro, Y., Fukuzumi, S., Kano, K., Takagi, K., and Ikeda, T. (1995) *J. Am. Chem. Soc. 117*, 1485−1493.
7. Van der Palen, C. J. N. M., Slotboom, D. J., Jongejan, L., Reijnders, W. N. M., Harms, N., Duine, J. A., and Van Spanning, R. J. M. (1995) *Eur. J. Biochem. 230*, 860−871.
8. Van der Palen, C. J. N. M., Reijnders, W. N. M., De Vries, S., Duine, J. A., and Van Spanning, R. J. M. (1997) *Antonie van Leeuwenhoek 72*, 219−228.
9. Matsuzaki, R., Fukui, T., Sato, H., Ozaki, Y., and Tanizawa, K. (1994) *FEBS Lett. 351*, 360−364.
10. Chistoserdov, A. Y., Boyd, J., Mathews, F. S., and Lidstrom, M. E. (1992) *Biochem. Biophys. Res. Commun. 184*, 1226−1234.
11. Chistoserdov, A. Y., Chistoserdova, L. V., McIntire, W. S., and Lidstrom, M. E. (1994) *J. Bacteriol. 176*, 4052−4065.
12. Chistoserdov, A. Y., McIntire, W. S., Mathews, F. S., and Lidstrom, M. E. (1994) *J. Bacteriol. 176*, 4073−4080.
13. Gak, E. R., Chistoserdov, A. Y., and Lidstrom, M. E. (1995) *J. Bacteriol. 177*, 4575−4578.
14. Van Spanning, R. J. M., Van der Palen, C. J. N. M., Slotboom, D. J., Reijnders, W. N. M., Stouthamer, A. H., and Duine, J. A. (1994) *Eur. J. Biochem.* 226, 201−210.
15. Van Spanning, R. J. M., Wansell, C. W., Reijnders, W. N. M., Oltmann, L. F., and Stouthamer, A. H. (1990) *FEBS Lett. 275*, 217−220.
16. Husain, M., and Davidson, V. L. (1985) *J. Biol. Chem. 260*, 14626−14629.
17. Davidson, V. L. (1990) *Methods Enzymol. 188*, 241−246.
18. Van Spanning, R. J. M., Wansell, C. W., Harms, N., Oltmann, L. F., and Stouthamer, A. H. (1990) *J. Bacteriol. 172*, 986−996.
19. Mather, M. W., McReynolds, L. M., and Yu, C. H. (1995) *Gene 156*, 85−88.
20. de Vries, G. E., Harms, N., Hoogendijk, J., and Stouthamer, A. H. (1989) *Arch. Microbiol. 152*, 52−57.
21. Chang, J. P., and Morris, J. G. (1962) *J. Gen. Microbiol. 29*, 301−310.
22. Davidson, V. L., and Sun, D. (2002) *Methods Enzymol. 353*, 121−130.
23. Francis, R. T., and Becker, R. B. (1984) *Anal. Biochem. 136*, 509−514.
24. Berry, E. A., and Trumpower, B. L. (1987) *Anal. Biochem. 161*, 1−15.
25. Sahlin, M., Gräslund, A., and Ehrenberg, A. (1986) *J. Magn. Reson. 67*, 135−137.
26. Brudvig, G. W. (1995) *Methods Enzymol. 246*, 536−554.
27. Husain, M., and Davidson, V. L. (1986) *J. Biol. Chem. 261*, 8577−8580.
28. Herbaud, M. L., Aubert, C., Durand, M. C., Guerlesquin, F., Thony-Meyer, L., and Dolla, A. (2000) *Biochim. Biophys. Acta 1481*, 18−24.
29. Graichen, M. E., Jones, L. H., Sharma, B. V., van Spanning, R. J. M., Hosler, J. P., and Davidson, V. L. (1999) *J. Bacteriol. 181*, 4216−4222.
30. Husain, M., and Davidson, V. L. (1987) *J. Bacteriol. 169*, 1712−1717.
31. Gilmour, R., Goodhew, C. F., Pettigrew, G. W., Prazeres, S., Moura, I., and Moura, J. J. G. (1993) *Biochem. J. 294*, 745−752.
32. Gilmour, R., Goodhew, C. F., Pettigrew, G. W., Prazeres, S., Moura, J. J. G., and Moura, I. (1994) *Biochem. J. 300*, 907−914.
33. Hu, W., Van Driessche, G., Devreese, B., Goodhew, C. F., McGinnity, D. F., Saunders, N., Fulop, V., Pettigrew, G. W., and Van Beeumen, J. J. (1997) *Biochemistry 36*, 7958−7966.
34. Fulop, V., Ridout, C. J., Greenwood, C., and Hajdu, J. (1995) *Structure 3*, 1225−1233.
35. Arciero, D. M., and Hooper, A. B. (1994) *J. Biol. Chem. 269*, 11878−11886.
36. Shimizu, H., Schuller, D. J., Lanzilotta, W. N., Sundaramoorthy, M., Arciero, D. M., Hooper, A. B., and Poulos, T. L. (2001) *Biochemistry 40*, 13483−13490.
37. Fulop, V., Waitmough, N. J., and Ferguson, S. J. (2001) *Adv. Inorg. Chem. 51*, 163−204.
38. Prazeres, S., Moura, J. J., Moura, I., Gilmour, R., Goodhew, C. F., Pettigrew, G. W., Ravi, N., and Huynh, B. H. (1995) *J. Biol. Chem. 270*, 24264−24269.
39. Foote, N., Peterson, J., Gadsby, P. M., Greenwood, C., and Thomson, A. J. (1985) *Biochem. J. 230*, 227−237.

40. Arciero, D. M., and Hooper, A. B. (1994) *J. Biol. Chem. 269*, 11878−11886.
41. Chu, G. C., Couture, M., Yoshida, T., Rousseau, D. L., and Ikeda-Saito, M. (2000) *J. Am. Chem. Soc. 122*, 12612−12613.
42. Lloyd, E., Hildebrand, D. P., Tu, K. M., and Mauk, A. G. (1995) *J. Am. Chem. Soc. 117*, 6434−6438.
43. Lipscomb, J. D. (1980) *Biochemistry 19*, 3590−3599.
44. Ruf, H. H., Wende, P., and Ullrich, V. (1979) *J. Inorg. Biochem. 11*, 189−204.
45. Dawson, J. H., Andersson, L. A., and Sono, M. (1982) *J. Biol. Chem. 257*, 3606−3617.
46. Sono, M., and Dawson, J. H. (1982) *J. Biol. Chem. 257*, 5496−5502.
47. Sono, M., Hager, L. P., and Dawson, J. H. (1991) *Biochim. Biophys. Acta 1078*, 351−359.
48. Ojha, S., Hwang, J., Kabil, Ö., Penner-Hahn, J. E., and Banerjee, R. (2000) *Biochemistry 39*, 10542−10547.
49. Liu, Y., Moönne-Loccoz, P., Loehr, T. M., and Ortiz de Montellano, P. R. (1997) *J. Biol Chem. 272*, 6909−6917.
50. Leys, D., Backers, K., Meyer, T. E., Hagen, W. R., Cusanovich, M. A., and Van Beeumen, J. J. (2000) *J. Biol. Chem. 275*, 16050−16056.
51. Gaul, D. F., Gray, C. O., and Knaff, D. B. (1983) *Biochim. Biophys. Acta* 723, 333−339.

BI034243Q